

# Multilevel diffractive lens in the MWIR with extended depth-of-focus and wide field-of-view

Tina Hayward,<sup>1</sup> Noor Qadri,<sup>2</sup> Nicole Brimhall,<sup>3</sup> Freddie Santiago<sup>2</sup> & Rajesh Menon<sup>1,3,\*</sup>

<sup>1</sup>Department of Electrical & Computer Engineering, University of Utah, 50 Central Campus Dr., Salt Lake City, UT 84112, USA.

<sup>2</sup>US Naval Research Laboratory, Washington, DC 20036, USA

<sup>3</sup>Oblate Optics, Inc., San Diego, CA 92130, USA

\*rmenon@eng.utah.edu

## 1. Issues of focusing efficiency reports in metaleenses in the MWIR:

The focusing by a diffractive lens (including metaleenses) is illustrated in Fig. S1. In all cases, the power in the focal spot is measured by placing a power meter in the place of the +1 order focus. The incident power is measured by placing the power meter in front of the lens and an iris of the same size as the lens is used. The ratio is typically reported as focusing efficiency.

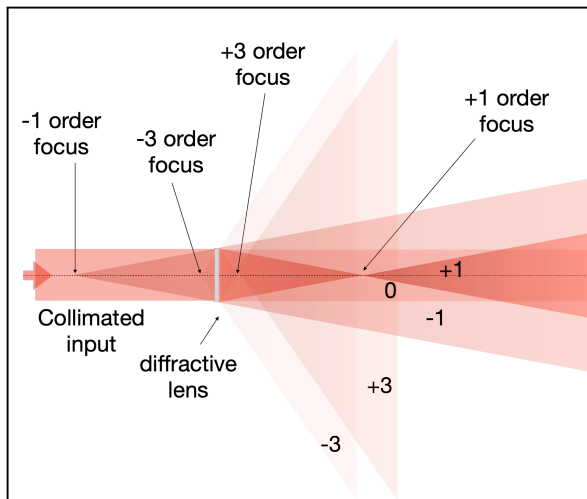


Figure S1: How a diffractive lens focuses?

The problem arises because for the first measurement an iris is used to restrict the area to the focal spot, but in all cases, this area is many times larger than the FWHM of the focal spot. This conflates the first- and zero-order diffracted powers and thereby greatly over-estimates focusing efficiency. As an example, in ref [1] the FWHM of the focused spot is  $\sim 2\mu\text{m}$ , but an iris of diameter  $200\mu\text{m}$  is used for measuring the focusing efficiency. And in ref [2], no iris is used at all.

## 2. Fabrication details:

A silicon MDL was fabricated using an intrinsic silicon wafer with a 100 mm diameter, 525  $\mu\text{m}$  thickness,  $<100>$  orientation, and a resistivity  $>10,000 \text{ Ohmcm}$  from MSE Supplies LLC. Three sequential lithography and RIE (reactive ion step) steps were used to pattern the samples. First, a surface adhesion promoter was applied by dipping the samples for 60 sec in SurPass

4000 from DisChem, Inc., followed by a 30 sec water rinse. A Shipley S1811 photoresist layer was spun at 3000 RPM, baked at 115 °C for 1 min, and then exposed with the Heidelberg MLA150 (405 nm laser at a dose of 80 mJ/cm<sup>2</sup>). The resist was developed for 60 sec. in MICROPOSIT MF CD26 developer from Rohm And Haas Electronic Materials LLC. After developing, the samples were rinsed in water for 60 sec. The used RIE was an ICP (induction coupled plasma) PlasmaPro 100 from Oxford Instruments. The silicon was etched with a gas mixture of SF<sub>6</sub>, C<sub>4</sub>F<sub>8</sub> and Ar (flow-rates 26/54/20 sccm) at room temperature of 20 °C. The chamber pressure was 19 mTorr, the forward power 15 W, and 825 W ICP, resulting in a gas-mixture ionization voltage of 370 V. The RIE process lasted for 800 sec with a silicon etch rate of ~ 4.4 nm/sec. After ICP-RIE, the sample was rinsed with acetone to remove the remaining resist; followed by a 60 sec. oxygen plasma clean (20 °C, 30 mTorr, 20 sccm O<sub>2</sub>, forward power 100 W).

For grayscale optical lithography of the FZP, we used a 2-inch diameter, 430um-thick double-side polished sapphire wafer as the substrate. It was spin coated with a positive-tone photoresist (ma-P1275, Microresist Technology GmbH) at 1000rpm for 60s followed by baking on a hot-plate at 20degC (20min), ramp up to 60degC (10min), held at 60degC (10min), ramp up to 100degC (10min) and held at 100degC (1min) followed by a multi-day cool-down. This resulted in a total photoresist thickness of ~ 15\um. The absolute total thickness is not critical for our fabrication as long as it is larger than the maximum ring height (6um). After a calibration step that has been described elsewhere, the FZP geometry was patterned using a laser pattern generator (DWL66+, Heidelberg Instruments GmbH). After exposure, the photoresist was developed in AZ 300 MIF developer (EMD Performance Materials Corp.) for 5 minutes.

### 3. Metrology results:

The average absolute height error for the FZP was 778 nm, but the standard deviation was 1.49 μm. The relatively low average error and the high standard deviation value each stem from a combination of the average step value and the general errors in the fabrication. The tallest portions of the design were thinner than the desired feature size, which caused the average center value to be located half-way down the feature rather than at its (too-thin) peak. The low average value caused several points of error that were far below zero, which averaged out the points where the error was almost 1 μm, but increased the standard deviation. This is clearly shown in Fig. S2 (a), where the red line represents the expected heights of the FZP, the blue line represents the measured heights, and the black circles represent the averaged center of each ring. Note that the tall flat region in the measured data represents the untouched photoresist outside the fabricated design. Fig. S2 (b) shows a graph of the error between the measured and expected heights.

The average error and standard deviation of the MDL were 504 nm and 1.08 μm, respectively. Because the heights were only measured 1.1057 μm from each other and the feature size was only 4 μm, only the center points of the features, shown in Fig. S2 (c), were considered for the error calculation. The resulting error graph is shown in Fig. S2 (d).

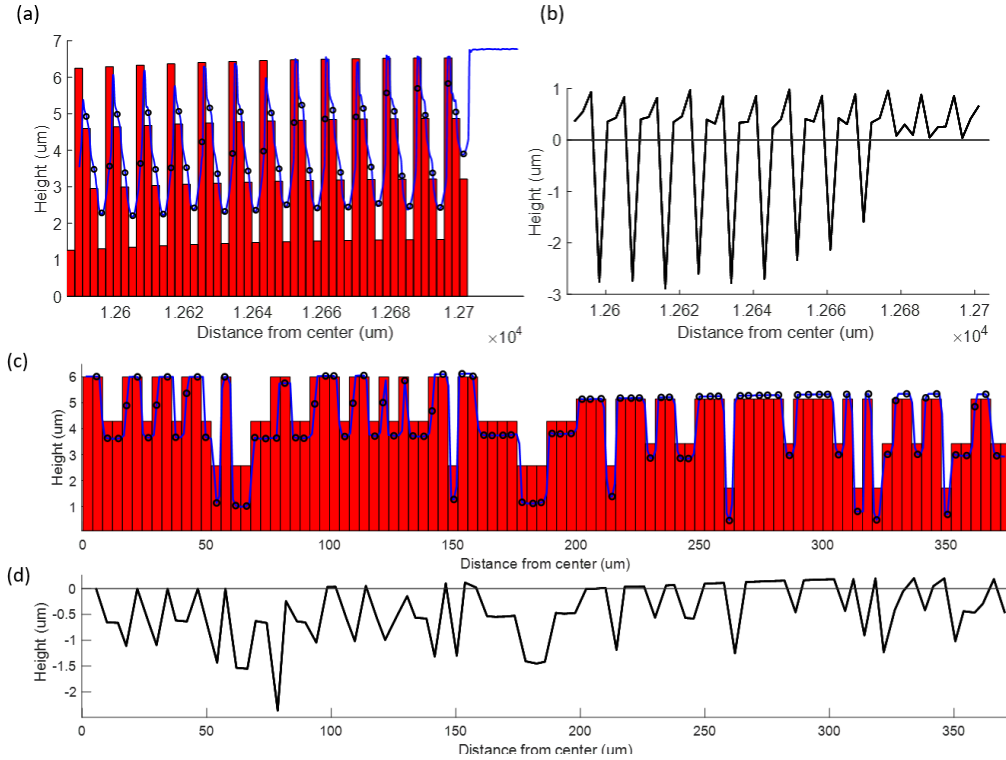


Fig. S2: Measured height errors for the FZP (a, b) and the MDL (c,d).

#### 4. Simulations of impact of height errors:

The impact of ring-height errors were studied by simulating the on-axis PSF of ten lenses, each with a random set of height errors taken from a normal distribution of mean and standard deviation matching the measurements in section 2 above. The results for the MDL and the FZP are summarized in Figs. S3 and S4, respectively.

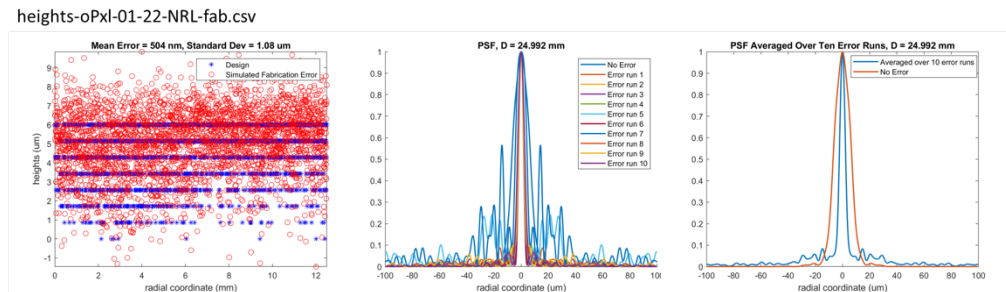


Figure S3: Impact of ring-height errors for the MDL.

Optimized\_design\_4um\_Fresnel\_maP.csv

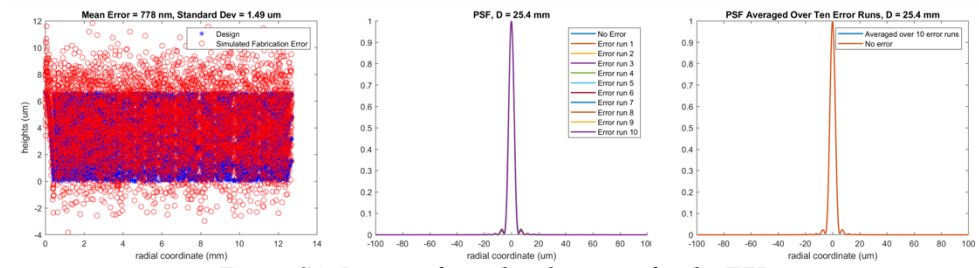
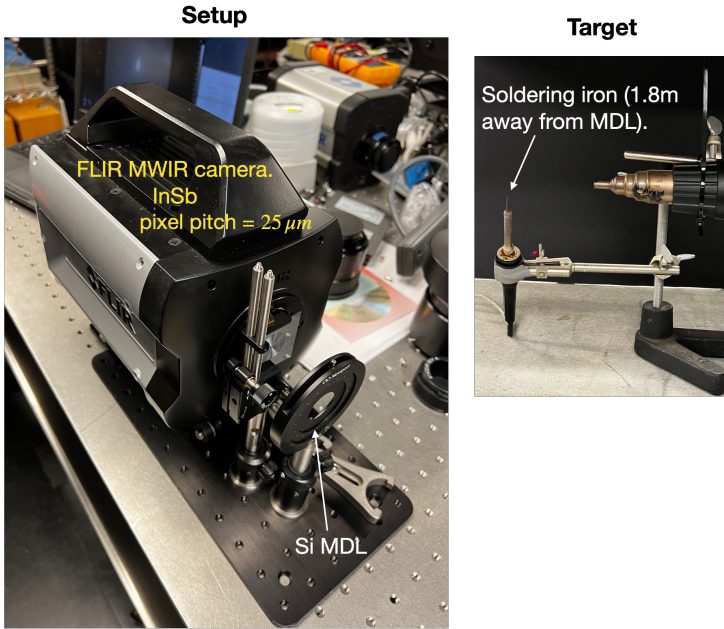


Figure S4: Impact of ring-height errors for the FZP.

## 5. Imaging Experiments:



The soldering iron is 6 feet away from the lens, and the lens is 2.2" from the housing edge for SC6000 FLIR (face of camera is 1.549"/39.3mm away from FPA).

Figure S3: Imaging soldering iron. Photographs of system and target.

Siemens chart image 0.5m away from MDL.

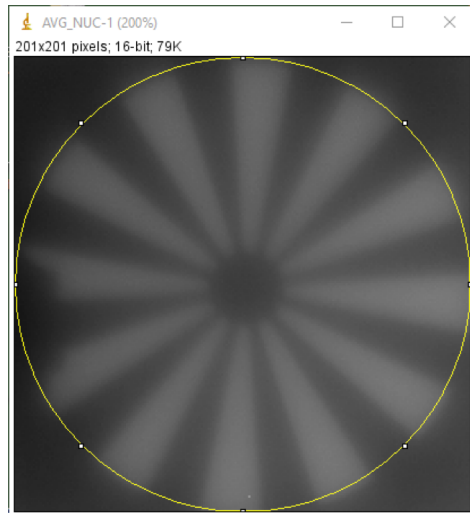


Figure S4: The Siemens target was 0.5 m away, and the dewar window is 19.4mm from FPA on that sensor (SCD Pelican D, f1/5, 640x512, 15um pitch, 3-5um response, InSb array).

**Target 2" from Photoresist lens on sapphire, lens pressed into the housing of FLIR SC6000 (Housing 1.549"/39.3mm from FPA)**

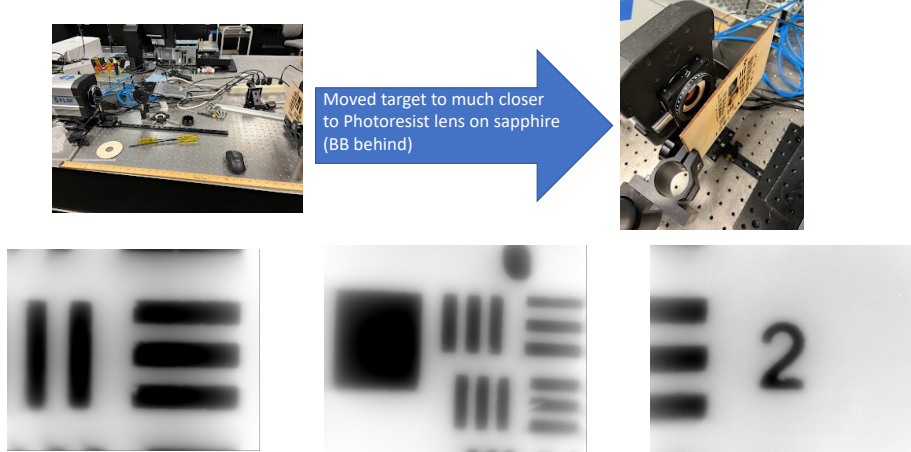


Figure S5: Imaging the AF resolution chart.

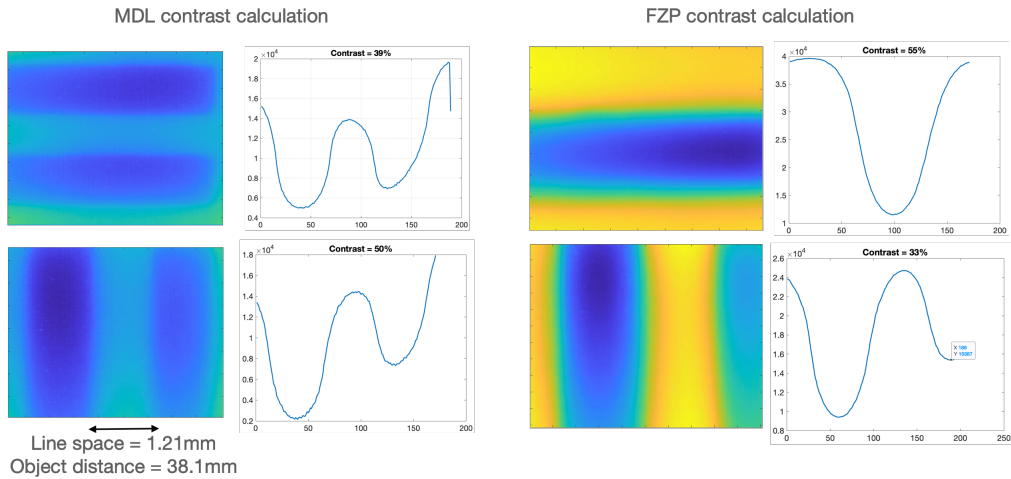
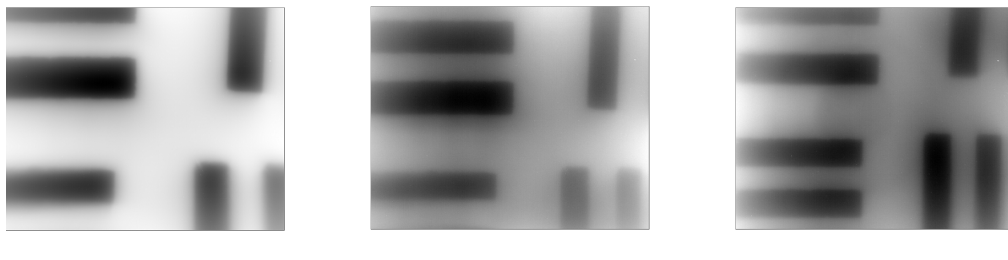


Figure S6: Calculation of image contrast.

**Target 1.5" from each lens, lens pressed into the housing of FLIR SC6000  
(Housing 1.549"/39.3mm from FPA)**



Group 4, -2: Horizontal top left/Vertical on top right) bars:  
Width 11.46 mm, 2.78mm height, 1.58 mm spacing

Group 5, -2: Horizontal bottom left/vertical bottom right: width  
10.63 mm, 2.59 mm height, 1.21 mm spacing

Figure S7: Details of imaging the AF resolution chart.



*Figure S8: Soldering iron target 8" from Si auto-align lens pressed into the housing of FLIR SC6000 (housing 1.549"/39.3mm from FPA).*

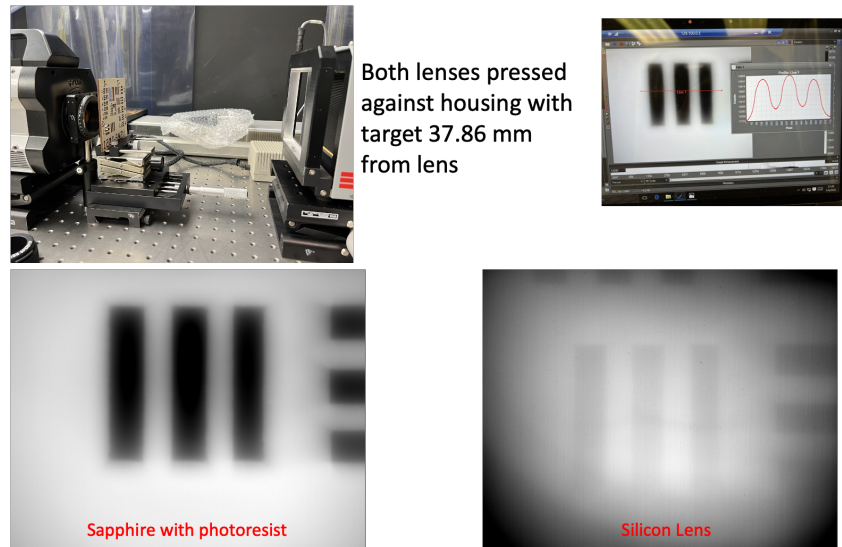


*Figure S9: Additional images of AF resolution chart.*

#### 6. Comparison of weights of lenses:

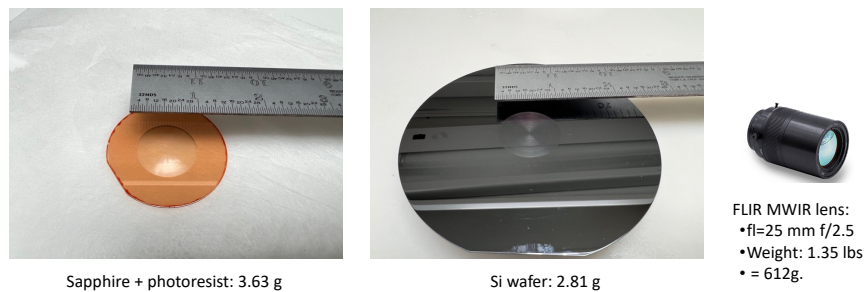


*Figure S10: Comparing the weights of the FZP (left), MDL (center) and a conventional refractive imaging system (right). The refractive has a slightly larger f# (f/2.5 vs f/1 for the MDL), so this is a more conservative comparison relative to the flat lenses.*

## 7. Field-of-view Measurements:

Figure S11 shows the schematic of the experiment used for the FOV measurements and the results are summarized in Fig. 3e in the main text.

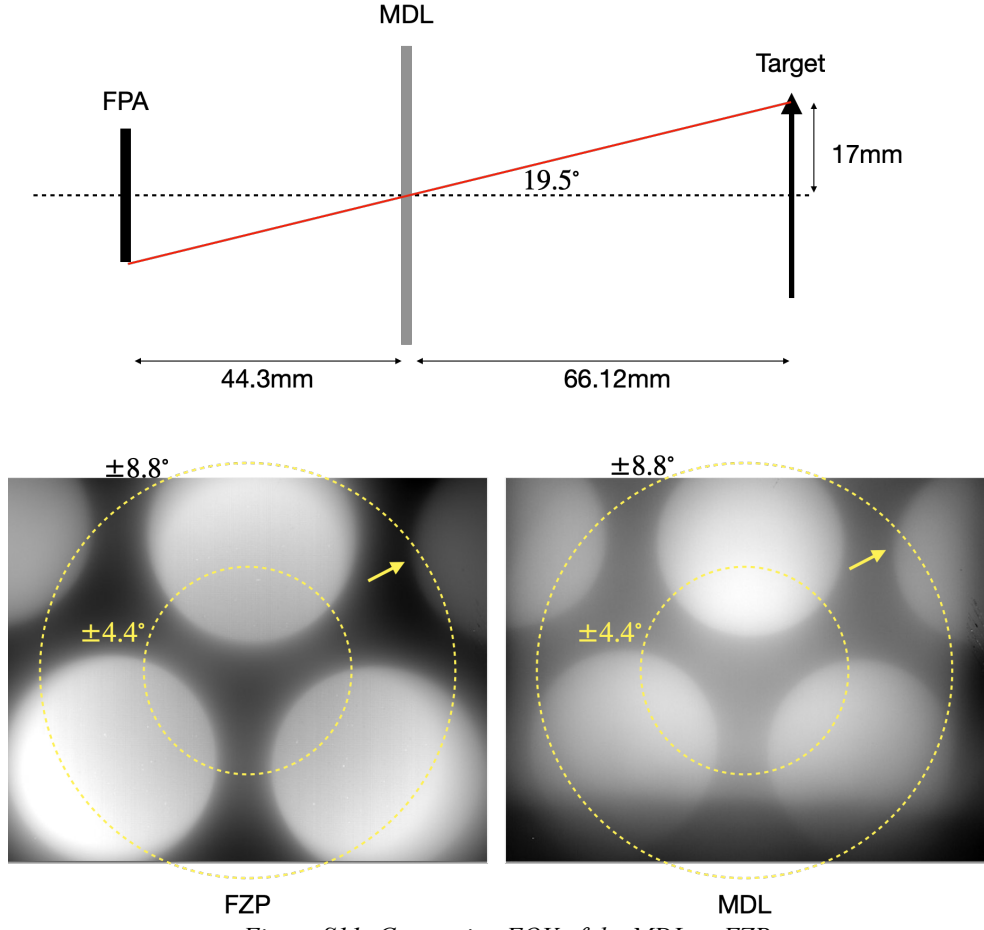


Figure S11: Comparing FOV of the MDL vs FZP.

## 8. Efficiency Measurements:

There are four steps for the efficiency measurements as summarized in Fig. S12. In step I, the incident power ( $P_{inc}$ ) is measured by placing the power meter (Ophir 30A-BB-18, diameter = 17.5mm) in front of the lens. In step II, the transmitted power ( $P_t$ ) is measured by placing the power meter right after of the lens. In step III, the power meter is placed in the designed focal plane ( $P_F$ ). In step IV, the power meter is placed in a far plane to measure the 0-order power ( $P_0$ ). In all cases, the illumination should ideally be a collimated laser beam. However, we didn't have access to this laser, so an extended black-body source placed far away from the lens was used. A filter centered at  $3.9\mu\text{m}$  was used between the black-body and the lens. Then, the transmission is calculated as  $P_t/P_{inc}$ . The integrated efficiency was computed as  $(P_F-P_0)/P_{inc}'$ , [3] where  $P_{inc}' = P_{inc} \times (\text{area of lens})/(\text{area of power-meter})$ . Here, we assumed that the lens is larger than the power meter. An iris may be placed in front of the power meter, but it is not

necessary. Detailed discussion of the integrated focusing efficiency is available in this important ref [3].

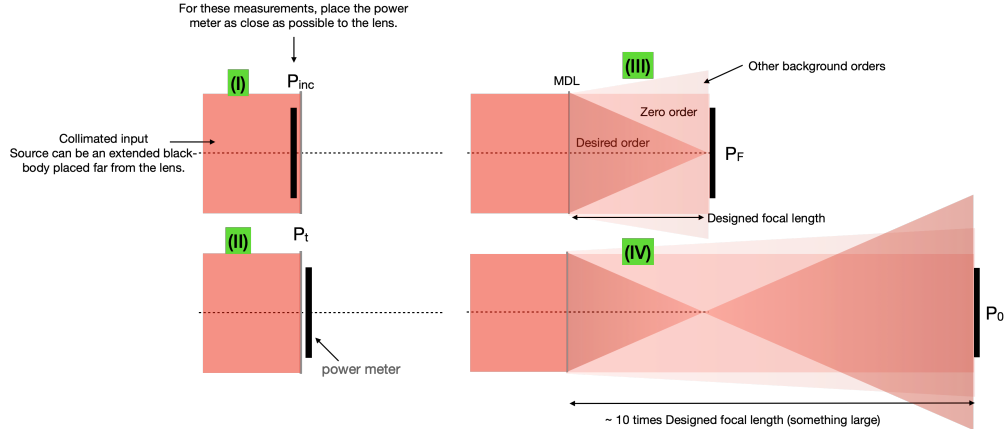


Figure S12: Steps for measuring the transmission and integrated focusing efficiencies [3].

Table S1: Measured efficiency values. The transmission was removed for the integrated focusing efficiency and the 0-order efficiency. Raw power values are in table S2.

Lens	Si MDL	PR on Sapphire FZP
Transmission (@ 4μm)	54%	78%
Integrated focusing efficiency	19%	22%
Fraction of incident power in zero order	51%	32%

The integrated focusing efficiency was measured using an extended blackbody source placed 584mm away from each lens. The power meter was first placed at the nominal focus (distance from lens of 25mm) and then moved to a far distance from lens (813mm away). The first measurement gives the focused power and the background, while the second measurement provides the zero-order power (which is assumed to be the primary contributor to the background within the aperture of the power meter). In other words, higher diffraction orders do not make it inside the power meter. Lastly, the incident power was measured by removing the lens and replacing it by the power meter. In all cases, a filter centered at 3.9μm was used (this was the closest wavelength that we had to the nominal design wavelength). The integrated focusing efficiency was then computed as:  $(\text{total power at focus} - \text{power in 0-order}) / (\text{incident power} \times \text{transmission})$ . The denominator was scaled by transmission to separate the Fresnel reflection losses from the diffraction losses. The transmission was measured using a separate experiment with the 4μm laser and the measured values are in table S3.

Table S2: Measured power values using blackbody.

Lens	Si MDL	PR on Sapphire FZP
$P_F$	1.4mW	1.7mW
$P_{\text{inc}}$	4mW	4mW
$P_0$	1.1mW	1mW

Table S3: Measured power densities using 4μm laser for transmission.

Lens	Si MDL	PR on Sapphire FZP
$P_{\text{inc}}$	0.3043 W/cm <sup>2</sup>	0.28 W/cm <sup>2</sup>
$P_t$	0.5603 W/cm <sup>2</sup>	0.3607 W/cm <sup>2</sup>

## References

1. M. Y. Shalaginov, S. An, F. Yang, P. Su, D. Lyzwa, A. M. Agarwal, H. Zhang, J. Hu, and T. Gu, "Single-element diffraction-limited fisheye metalens," *Nano Lett.* 20, 7429–7437 (2020).
2. J. Engelberg, C. Zhou, N. Mazurski, J. Bar-David, A. Kristensen, and U. Levy, "Near-ir wide-field-of-view huygens metalens for outdoor imaging applications," *Nanophotonics* 9, 361–370 (2020).
3. Dale A. Buralli and G. Michael Morris, "Effects of diffraction efficiency on the modulation transfer function of diffractive lenses," *Appl. Opt.* 31, 4389-4396 (1992).